

NACA TM 1410

7962

# NATIONAL ADVISORY COMMITTEE FOR AERONAUTICS

TECHNICAL MEMORANDUM 1410

THEORY AND EXPERIMENTS ON SUPERSONIC

AIR-TO-AIR EJECTORS

By J. Fabri and J. Paulon

Translation of "Théorie et expérimentation des éjecteurs  
supersoniques air-air." O.N.E.R.A.  
Note Technique No. 36, 1956.



Washington

September 1958

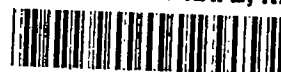
AFMDC  
TECHNICAL LIBRARY  
AFL 2811

0144482



TECH LIBRARY KAFB, NM

TM  
1410  
C-1



## THEORY AND EXPERIMENTS ON SUPERSONIC

## AIR-TO-AIR EJECTORS\*

By J. Fabri and J. Paulon

## I. INTRODUCTION

Ejectors have been employed in industry for a very long time; most frequently, however, their use has been restricted to rather special cases of operation. The extrapolation of recorded performance under these conditions did not permit achieving with certainty the design of a configuration of large power which was supposed to have satisfactory extraction capacity over a wide range of mass flows and compression ratios. Systematic testing and the theory of high-compression ejectors (that is, ejectors whose primary flow is supersonic) have been taken up more recently in various countries (refs. 1, 2, and 3). The elementary theory, which we have proposed (ref. 4) for interpretation of the test performance in the case of cylindrical mixers, is essentially aerodynamical. It determines the suction characteristics of a supersonic ejector by the conditions of aerodynamic compatibility between the existing flows, written in simplified geometrical representations of the configuration and independent of any consideration of the viscosity and diffusion phenomena which establish and maintain the regime. Due to this fact, it does not permit representing the influence of certain important parameters like the relative length of the mixer or the reciprocal positions of the primary and secondary jets. The actual agreement of the results of this theory with the measured results, when it is applied to predicting the operation of installations for the optimum empirical values of the above parameters, justifies fully the viewpoint we adopted; besides, a reduced number of diagrams permits, with sufficient accuracy, the achievement of a preliminary design for an ejector corresponding to a given set of requirements, or the discussion of the extraction possibilities by a given source of primary flow (ref. 5).

We thought it of interest to present here an experimental verification of this entire theory, taking into consideration (as we did previously in the special case of the regime of zero induced mass flow in ref. 6) the load losses due to the friction at the wall in the subsonic part of the motion.

---

\*"Théorie et expérimentation des éjecteurs supersoniques air-air."  
O.N.E.R.A. Note Technique No. 36, 1956.

## II. TEST APPARATUS

The experimental results presented below have been obtained with the aid of a device of very small dimensions whose input supply may be obtained from the compressed air of the city distribution system or, for high generating pressures, from commercial high-pressure bottles. The mounting is done by means of metal bodies of revolution, screwed end to end. They are easy to interchange, thus permitting various geometrical configurations. In each of them (fig. 1), a primary settling chamber supplies a supersonic nozzle after the primary flow has passed through a convergent tube and a cylindrical inlet channel. The secondary circuit which drains in the surrounding atmosphere includes a mass-flow meter (convergent entry or calibrated diaphragm), a regulating valve for the mass flow, and a settling chamber. The two coaxial flows make contact (plane 1) in the cylindrical mixing tube, of the length  $l$  which is followed (plane 2) by a divergent portion with half-angle  $\alpha$ , the end of which (plane 3), opens into the atmosphere at the pressure  $p$ . Two mixers of different diameters can be used in the apparatus.

Among the supersonic nozzles used, whose main dimensions are reproduced in figure 2, the majority, such as B, C, D, E are geometrically constituted (for ease of manufacture) of two truncated cones which have a common base at the throat. They produce in their exit section a flow of conical character; in the case of the nozzle E<sub>1</sub>, the divergent part of which is doubly curved, the exit flow is, on the contrary, reasonably uniform.

The generating pressures of the two flows, knowledge of which is necessary for the calculation of the primary mass flow and of the compression ratio of the ejector, respectively, are obtained with the aid of pressure taps at the wall of the settling chambers of the two flows. This measurement does not present any particular difficulty; nevertheless, due to the load losses in the inlet flow, which are practically independent of the configuration considered, the generating pressure of the primary supersonic flows represents only 96 percent of the inlet pressure, measured in the settling chamber upstream. This last pressure which we consider below, for convenience of reading, as characteristic for the primary flow, must therefore be corrected in the numerical applications.

### III. OPERATIONAL SCHEME OF AN EJECTOR

The one-dimensional description of the aerodynamic operation of the ejectors used is greatly simplified due to the care we have taken in placing, as much as possible, the exit section of the primary flow in the cylindrical part of the mixer. However, the scheme of calculation differs from the one previously described (ref. 4) as a result of the need - so that the calculation should follow the measured results with more precision - on the one hand, to take into account the load losses due to the wall friction in the subsonic part of the flow, and on the other hand, in view of the very small scale of the apparatus, not to neglect the wall thickness of the primary nozzle at its end in the different aerodynamic balances. Finally, for operations at low generating pressures, we assumed that the primary flow did not completely fill its nozzle, and the corresponding calculations were performed by generalization of a method described elsewhere (ref. 6) for vacuum pumps without secondary mass flow.

We take as unity the outlet section  $S$  of the primary nozzle (figs. 1 and 4) and denote by  $\lambda$  the cylindrical section of the mixer and by  $\lambda' - 1$  (slightly smaller than  $\lambda - 1$ ) the outlet section of the secondary flow;<sup>1</sup> we utilize, furthermore, the geometrical parameters  $\lambda_*$ , the ratio of the mixer cross section to the cross section at the throat of the primary nozzle,<sup>2</sup> and  $\sigma$ , the ratio of the end sections of the outlet-divergent tube. The aerodynamic description of the motion is given for every flow by means of the critical Mach number  $M_*$ , the ratio of the local mean velocity to the critical sonic velocity  $a_*$  of the flow considered. The subscripts 1, 2, and 3 correspond to the three planes of reference already indicated; we reserve the subscript 0 for denoting the contingent separation cross section of the primary flow in the driving nozzle and the subscript i for the quantities of the generating conditions. A prime designates the primary flow and a double prime the secondary flow when these two flows are distinct; the absence of a prime corresponds to the hypothesis of a homogeneous mixing of the two flows. We assume, furthermore, the specific heats of the two gases before and after the mixing to be constant (designating the fundamental grouping connected with the ratio of the specific heats by  $m^2 = (\gamma + 1)/(\gamma - 1)$ ), and we assume that, in the entire series of tests performed, the primary and secondary generating temperatures are constant and equal.

---

<sup>1</sup>The calculation of  $\lambda'$  is easily performed, starting from the terminal dimensions given in figure 2.

<sup>2</sup>Since the primary nozzles have very similar throat surfaces, the parameter  $\lambda_*$  assumes, in practice, in all our configurations only two different values, according to the mixer used.

### 3.1. Supersonic Regimes

When the generating pressure of the primary flow is sufficiently large, with respect to the back pressure of the medium into which the ejector discharges, the supersonic flow, started in the primary tube, subsists in the mixer and the induced fluid itself is entrained at high speed (fig. 3(a)).<sup>3</sup> It is then clear that the pressure conditions downstream do not impose any limitation of mass flow on the mixer, and the induced mass flow is equal to the maximum admissible in the coexistence of the two streams. The latter holds beyond section 1 for a certain length. If the development of the secondary flow, generally subsonic, can be described, with good approximation, within the classical hypothesis of motions in sections, that of the supersonic primary flow depends on the method of the characteristics. But when the pressure  $p_1''$  of the secondary flow is lower than the pressure  $p_1'$  of the primary flow at the nozzle exit, the latter spreads in the mixing tube and attains in the section of maximum expansion (subscript e) a quasi-uniform structure. This occurs in such a manner that it is possible to consider between the planes 1 and e a universal one-dimensional and isentropic behavior of the two fluids, since the local continuity of the pressures on the surface of the two jets evidently does not entail the equality of the mean pressures  $p_e'$  and  $p_e''$ .

The finite thickness of the walls of the primary nozzle in its end section entails the existence of a wake, very obvious in the shadowgraphs. One can assume that, over the small length which separates the planes 1 and e in the mixer, the section  $\lambda - \lambda'$  of this wake is in practice not supplied by either flow whose mixing is still negligible. If  $v$  (fig. 4) designates the expansion section of the primary jet, we can write the equations of continuity for each flow in the form

$$v = \frac{M_{*1}'}{M_{*e}'} \left( \frac{m^2 - M_{*1}'^2}{m^2 - M_{*e}'^2} \right)^{\frac{1}{\gamma-1}}, \quad \frac{\lambda' - v}{\lambda' - 1} = \frac{M_{*1}''}{M_{*e}''} \left( \frac{m^2 - M_{*1}''^2}{m^2 - M_{*e}''^2} \right)^{\frac{1}{\gamma-1}} \quad (1)$$

---

<sup>3</sup>In the configurations represented in shadowgraphs in figure 3, the primary flow issues, at the mean Mach number  $M_{*1}' = 1.78$ , from a plane divergent nozzle (dihedral of  $10^\circ$ ) into a plane cylindrical mixing tube with a ratio of sections  $\lambda = 2.61$ . The four views correspond to an equal opening of the secondary valve.

where the pressures are those of the isentropic expansion

$$\frac{p_e'}{p_1} = \left( \frac{m^2 - M_{*e}'^2}{m^2 - M_{*1}'^2} \right)^{\frac{\gamma}{\gamma-1}}, \quad \frac{p_e''}{p_1} = \left( \frac{m^2 - M_{*e}''^2}{m^2 - M_{*1}''^2} \right)^{\frac{\gamma}{\gamma-1}} \quad (2)$$

If we then apply to each of the two flows the momentum theorem between the planes 1 and e, we note that the integrals of the pressures on the primary and secondary faces of the wake are opposite according to the condition of local continuity of the pressures, and we obtain, by addition, the universal relationship

$$\begin{aligned} p_1' \frac{1 + M_{*1}'^2}{m^2 - M_{*1}'^2} + (\lambda' - 1) p_1'' \frac{1 + M_{*1}''^2}{m^2 - M_{*1}''^2} = \\ \nu p_e' \frac{1 + M_{*e}'^2}{m^2 - M_{*e}'^2} + (\lambda' - \nu) p_e'' \frac{1 + M_{*e}''^2}{m^2 - M_{*e}''^2} \end{aligned} \quad (3)$$

Introducing then the condition of optimum operation indicated at the beginning of this section, for instance,  $M_{*e}'' = 1$ , we can - for given values of  $p_1'$ ,  $M_{*1}'$ ,  $\lambda'$  - solve the five equations (1), (2), and (3) with respect to the variables  $\nu$ ,  $p_e'$ ,  $p_e''$ ,  $M_{*e}'$ , and  $M_{*e}''$ , and deduce from them the suction capacity of the apparatus. The fundamental nondimensional characteristic of an ejector is then obtained by representing the ratio  $\mu$  of the secondary to primary mass flows as a function of the ratio  $\tilde{\omega}$  of the extraction pressure  $p_1''$  to the back pressure downstream  $p$

$$\left. \begin{aligned} \mu &= (\lambda' - 1) \frac{p_1''}{p_1'} \frac{M_{*1}''}{M_{*1}'} \left( \frac{m^2 - M_{*1}''^2}{m^2 - M_{*1}'^2} \right)^{\frac{1}{\gamma-1}} \\ \tilde{\omega} &= \frac{p_1''}{p} \left( \frac{m^2}{m^2 - M_{*1}''^2} \right)^{\frac{\gamma}{\gamma-1}} \end{aligned} \right\} \quad (4)$$

3.1.1. - When  $p_1''$  is greater than  $p_1'$ , the primary jet is initially convergent (fig. 3(b)), and the secondary mass flow is limited only by the aerodynamic blocking of the section  $(\lambda' - 1)$  of the supply conduit. The condition for optimum operation, therefore, becomes  $M_{x_1}'' = 1$ , and we then have in the  $(\mu, \tilde{\omega})$  diagram the linear characteristic of the saturated supersonic regime

$$\mu = \tilde{\omega}(\lambda' - 1) \frac{p}{p_1'} \frac{1}{M_{x_1}'} \left( \frac{m^2 - 1}{m^2 - M_{x_1}'^2} \right)^{\frac{1}{\gamma-1}} \quad (5)$$

which is joined continuously to the representative branch of the pure supersonic regimes, represented parametrically by equation (4). The slope of the straight lines (eq. (5)) is inversely proportional to the primary generating pressure; nevertheless, it is quite clear that the mass flow entrained by an ejector operating in a saturated regime is, for a given value of  $\tilde{\omega}$ , completely independent of the pressure  $p_1'$ .

We shall finally note that, when the conditions of existence for these supersonic regimes are satisfied, the operation of the ejector is determined by the laws of the aerodynamics of perfect fluids; the viscosity phenomena have only the effect of delaying more or less the appearance of these regimes and govern only the start of the phenomenon.

### 3.2. Mixed Regime

If we reduce the primary generating pressure, the supersonic mixer deenergizes itself partially by progressive increase of shock waves (fig. 3(c)); thus the entrainment takes place between two subsonic streams, and the induced mass flow is limited by the possibility of exit of the total flow which is supposed to be made uniform in velocity and pressure in the end section of the mixer. The configuration of the motion depends, thus, closely on the characteristics of the conduits, already defined from the geometrical viewpoint; the determination from the mechanical viewpoint will be achieved by the supplementary parameter of the mean turbulent-friction coefficient  $f$  of the gas at the wall. The uniformity of the subsonic stream issuing from the two flows is then supposed to be achieved, owing to a sufficient settling length  $l$  in the entrance section of the diffuser. The mean load loss of the flow between the planes 1 and 2 may be represented, within the framework of the one-dimensional theory of the turbulent flows in the conduits, by the approximate formula

$$\left| \delta p \right|_1^2 = -f \frac{\rho_2 a_*^2 M_{*2}^2}{2} \xi \quad (6)$$

where  $\rho$  denotes the specific mass of the fluid and  $\xi$  the ratio of the lateral surface of the stream to its transverse section  $\lambda S$ , here, for instance,  $4l/D$ ;  $D$  is the diameter of the mixing tube.

The continuity and the momentum equations are then written, between sections 1 and 2 of the mixing tube (ref. 7)

$$\left. \begin{aligned} \frac{p_1' M_{*1}'}{m^2 - M_{*1}'^2} + (\lambda' - 1) \frac{p_1'' M_{*1}''}{m^2 - M_{*1}''^2} &= \lambda \frac{p_2 M_{*2}}{m^2 - M_{*2}^2} \\ \frac{p_1' (1 + M_{*1}'^2)}{m^2 - M_{*1}'^2} + p_1'' \left[ (\lambda' - 1) \frac{1 + M_{*1}''^2}{m^2 - M_{*1}''^2} + \frac{(\lambda - \lambda')}{m^2} \right] &= \\ \lambda \frac{p_2 \left[ 1 + \left( 1 + \frac{f\xi}{2} \frac{m^2 + 1}{m^2} \right) M_{*2}^2 \right]}{m^2 - M_{*2}^2} & \end{aligned} \right\} \quad (7)$$

They permit deduction of the secondary operational conditions ( $p_1''$ ,  $M_{*1}''$ ) from the parameters ( $p_1'$ ,  $M_{*1}'$ ) of the primary flow at the exit of the driving nozzle when ( $p_2$ ,  $M_{*2}$ ) are disposed of. These quantities are calculated from ( $p_3$ ,  $M_{*3}$ ) by means of equations which represent, on the one hand, the continuity of the mass flow between the planes 2 and 3

$$\sigma = \frac{p_2}{p_3} \frac{M_{*2}}{M_{*3}} \frac{m^2 - M_{*3}^2}{m^2 - M_{*2}^2} \quad (8)$$

and, on the other hand, the expansion of the pressures in the diffuser between these same sections. When, in a conical nozzle with the opening  $\alpha$ , the load loss due to the friction has, per unit length, the elementary



form (eq. (6)), we obtain (ref. 8), putting  $\zeta = 2 \tan \alpha / f \gamma$ , and after combination with (eq. (8))

$$\sigma = \frac{M_{*2}}{M_{*3}} \left[ \frac{\zeta m^2 - (\zeta + m^2 - 1) M_{*2}^2}{\zeta m^2 - (\zeta + m^2 - 1) M_{*3}^2} \right]^{\frac{\zeta - 1}{(\gamma - 1)\zeta + 2}} \quad (9)$$

As to  $(p_3, M_{*3})$ , the first is fixed by the exit condition of the flow

$$p_3 = p$$

and the other may be chosen arbitrarily, so as to describe the overall mixed characteristic of the ejector. The reduced variables  $(\mu, \tilde{\omega})$  are always calculated according to their definition (eq. (4)) which does not present any particular difficulty. Nevertheless, it is important to select a convenient value for  $f$ . The turbulent friction of the air at the smooth walls of the mixer corresponds to a coefficient  $f$ , which the universal relationship (ref. 9)

$$f^{-1/2} = 4 \log Rf^{1/2} - 0.4$$

or its approximate representations permit calculating from the transverse Reynolds number  $R$  of the stream. According to this formula, the values of  $f$  relative to the flow in plane 2 change only slightly in our tests. For simplification, we performed the numerical calculations with the single mean value  $f = 0.0053$ .

### 3.3. Mixed Regime With Primary Separation

For still lower primary generating pressures, the aerodynamic character of the primary flow and, consequently, the suction characteristic of the pump are influenced by the geometrical form of the nozzle. In fact, the one-dimensional theory of nozzle would lead us normally to predict, as a mixed-operation limit for low generating pressures, the configuration in which equality would be attained between the secondary pressure  $p_1''$  and the pressure of the subsonic flow resulting from the primary flow through a straight shock under the conditions  $(p_1', M_{*1}')$ , for instance

$$\frac{p_1''}{p_1'} = \frac{m^2 M_{*1}'^2 - 1}{m^2 - M_{*1}'^2}$$

The operation would then become like that of a classical subsonic ejector. It is possible that this scheme could have some value when the driving nozzle is effectively subject to deenergization by increase of straight or more complex shock waves in the divergent tube. This possibility seems to be facilitated by the presence of an inflection point in the meridian of the latter. However, in the very frequent case of nozzles with conical divergent tubes, no straight-wave configuration appears, in general, to cause the deenergization of the primary flow. Rather, we observe (fig. 3(d)) the persistence of a supersonic jet issuing no longer from the edges of the nozzle but from a parallel interior of the divergent tube (plane 0). If we assume that the secondary pressure  $p_1''$  prevails in the whole unfilled part of the nozzle between the planes 0 and 1, we may, without changing at all the first of equations (7), modify the second in the following manner:

$$\lambda_0 p_0' \frac{1 + M_{*0}'^2}{m^2 - M_{*0}'^2} + p_1'' \left[ (\lambda' - 1) \frac{1 + M_{*1}''^2}{m^2 - M_{*1}''^2} + \frac{\lambda - (\lambda' - 1) - \lambda_0}{m^2} \right] =$$

$$\lambda p_2' \frac{1 + \left( 1 + f \frac{1 + m^2}{2m^2} \right) M_{*2}'^2}{m^2 - M_{*2}'^2} \quad (7')$$

where evidently

$$\lambda_0 = \frac{M_{*1}'}{M_{*0}'} \left( \frac{m^2 - M_{*1}'^2}{m^2 - M_{*0}'^2} \right)^{\frac{1}{\gamma-1}} \quad \frac{p_0'}{p_1'} = \left( \frac{m^2 - M_{*0}'^2}{m^2} \right)^{\frac{\gamma}{\gamma-1}} \quad (11)$$

According to a commonly assumed rule (ref. 10), the reversible pressure of the supersonic flow in the plane where separation occurs represents practically always the same fraction of the back pressure which acts downstream on the free surface of the jet. This amounts to saying that the oblique shock waves, across the flow is deflected toward the axis, and separates from the wall, have a reasonably constant compression

ratio. The mean experimental value of this ratio, near 2.5, according to the measurements made for the conical nozzles usually employed in rocket motors,<sup>4</sup> agrees rather well with the theoretical values of the compression ratios of the oblique waves which, within the range of Mach numbers considered, must cause the separation of the stream, due to their interaction with the boundary layer of the flow (ref. 11).

If we therefore adopt, for want of a more accurate rule, in our calculations the supplementary condition

$$p_1'' = 2.5p_0'$$

the number of unknowns contained in equations (7) to (7') remains at two (taking eq. (11) into account), and the solution may be sought in the manner indicated for the ordinary mixed regime, and abandoned as soon as

$$p_1'' \geq 2.5p_1' \quad (12)$$

### 3.4. Operational Characteristics

The group of theoretical mass-flow-pressure characteristics corresponding to the various supersonic and mixed regimes determines generally, for a given primary generating pressure and a given extraction pressure  $p_1''$ , different possible values for the entrained mass flow (fig. 5) from which the one that has been effectively realized must be chosen. It is evident that the possibilities of ejection into the surrounding atmosphere generally determine this choice. The supersonic regime is produced only if the mixed regime is very large; this simply amounts to choosing, between a supersonic or mixed characteristic, the one which, for a given extraction pressure, involves the lesser secondary mass flow. Conversely, the mixed regime with separation which prevails over the ordinary mixed regime - at least in certain nozzles with conical divergent tubes - under the conditions (eq. (12)), which involve only basic aerodynamics, is generally accompanied by an improvement in the ejector performance. (Cf. Rep. No. 44.)

---

<sup>4</sup>Nozzles which are generally adapted at expansion ratios  $p_1'/p_1''$  from 15 to 30 ( $1.6 \leq M_{x_1}' \leq 1.9$ ); besides, it is evident that the rule could not be applied to slightly supersonic flows (for  $M_{x_1}' = 1.37$ , the shock which gives a compression ratio of 2.5 is straight).

## IV. EXPERIMENTAL COMPARISONS

The experimental study of the ejectors with supersonic primary flow has been conducted so as to compare the experimental mass flows and pressures with the theoretical predictions. Furthermore, in the group of experimental findings which we present in this section, the curves plotted have always been obtained a priori from the equations of Report No. 3. Under the conditions we have specified, the points correspond to the measured results.

Figures 6 and 7 give, in all their apparent complexity, the family of suction characteristics of two similar ejectors for different values of the primary generating pressure. The second configuration is distinguished from the first by the addition of a diffuser. We observe, for  $p_1' = 5.5p$  in the two cases, and with the same performance, which is completely independent of the geometry downstream, first a pure, then a saturated supersonic regime. For  $p_1' = 4.5p$ , we observe both supersonic regimes when the mixer is provided with a diffuser and the mixed regime is followed by the saturated supersonic regime in the configuration without diffuser. For  $p_1' = 3.5p$ , we find the mixed regime going over into the saturated supersonic regime in the configuration containing the diffuser, and only the mixed regime in the other case. For  $p_1' = 2.5p$ , we observe the mixed regime with separation in both configurations.

On the whole, the agreement between calculation and tests is good, and the interpretation of the practical operational characteristics of an ejector is greatly facilitated by the theoretical discussion of the various regimes. Concerning the seemingly abnormal behavior of the experimental supersonic characteristic in the neighborhood of zero induced mass flow, we recall that the suction pressure  $p_1''$  in the secondary settling chamber may be identified, under these conditions, with the base pressure of the abrupt enlargement of the primary flow in the plane 1. In the case of the supersonic regime, this last pressure does not derive from an elementary aerodynamic calculation like the one presented here (ref. 6). Instead of an isentropic expansion, which by a tangential contact causes it to fill the entire cross section of the mixing tube, the primary free jet in its expansion has an impact on the cylindrical wall. There, according to a condition which is inversely analogous to that encountered in the study of separation of a boundary layer due to shock-wave action, the stability of the return in a guided jet is insured only when the compression ratio of the oblique waves stemming from the impact has a definite value. Feeding of the secondary jet, even at a very small mass flow, brings this phenomenon to a stop,

and the test points then agree again with the theoretical supersonic characteristics.

#### 4.1. Influence of the Length of the Mixer

The length of the mixing tube is an important parameter of the apparatus; it is convenient, for judging its influence on the extraction capacity of a given ejector, to study the variation of the extraction pressure obtained as a function of  $\xi$ , in mixed regime, for a given primary generating pressure and secondary mass flow (fig. 8). Between the very small values of  $\xi$ , at which the supersonic jet passes out into the surrounding atmosphere practically without action, and the very large values of  $\xi$  where the load losses of the flow, reorganized in the mixing tube, become important, the secondary generating pressure passes through a minimum for a value of  $\xi_m$  representing the lengthening of the cylindrical mixer. This causes, under the operational conditions considered ( $p_1/p$ ,  $M_{x1}$ ,  $\lambda$ ,  $\sigma$ ), the suction ratio  $\tilde{\omega}$  which is optimum for the adopted value of  $\mu$ . We see that the theory represents the variation of  $\tilde{\omega}$  very satisfactorily when  $\xi > \xi_m$ .

This limiting value depends, in fact, on the primary generating pressure. We see, for instance, that in mixed regime the more the supersonic phase of the driving jet is extended (figs. 3(c) and 3(d)), the higher its generating pressure, so that an increase of  $p_1/p$  causes, in this case, a reduction of the length of the mixer which is active in the subsonic mixing of the jets and, consequently, an increase of the minimum length  $\xi_m$ . One can also predict, for values of  $p_1/p$  high enough to make the supersonic regime prevail, that the value of  $\xi_m$  decreases again, to remain afterwards independent of  $p_1/p$ . In a general manner, we may assume that the theory always represents correctly the effect of lengthening the mixing tube for  $\xi$ -values higher than 50. Figures 9(a), (b), and (c) which represent, for three increasing primary generating pressures, the theoretical and experimental suction characteristics of ejectors which differ only in the length of their mixers, confirm this result. In figure 9(c), in particular, we see that, as predicted, the performance in the supersonic regime is not influenced by the length of the mixer as long as the latter is sufficient to make the establishment of the regime possible.

#### 4.2. Influence of the Terminating Diffuser

As in the preceding consideration regarding the relative length of the mixer (parameter  $\xi$ ), the terminating diffuser actually influences

the performance of the ejector only during operation in mixed regime; as a result, it governs the limit where the supersonic regimes appear. Figure 10 compares the mass flow-pressure characteristics of a given ejector for three different terminating configurations under identical primary conditions. We see how much an efficient diffuser facilitates establishment of the supersonic regime and thereby improves the suction characteristics of the ejector.

#### 4.3. Influence of the Cross Section of the Mixer

The ratio  $\lambda_*$  of the cross section of the mixer to that of the throat of the primary nozzle is a fundamental operational parameter. In figures 11 and 12, which correspond to figures 6 and 7, respectively, we represent the theoretical characteristics and the test points pertaining to the nozzle D operating in the mixer of large cross section. The definite improvement of the extraction conditions obtained when the mixer is provided with a diffuser is also correctly represented by the theory. Likewise, we note that, as a result of the large ratio of the sections, the supersonic regime appears now only for rather high generating pressures.

#### 4.4. Influence of the Primary Mach Number

In order to make evident the influence of the Mach number at the exit of the primary nozzle, we represent in figures 13(a), (b), (c), and (d) the theoretical and experimental performances of the nozzles B, C, D, and E for different primary generating pressures and the same mixer. We see that the less rapid nozzles, B and C, maintain mixed behavior at low generating pressures, whereas the separated regime prevails in the nozzles D and E. If, in this last case, the test points follow the theoretical curves rather irregularly, we must not forget that the corresponding regimes easily become more unstable than those in which the nozzles are completely energized. On the other hand, the empirical rule (eq. (12)) adopted for fixing the cross section of separation certainly does not have the universal character which we assume it to have in order to simplify the calculations.

Figure 14 compares the characteristics of the nozzles E and E<sub>1</sub>. These nozzles, which differ only by the geometrical form of their divergent tube and, consequently, by their tendency to show separations at the instant of their deenergization, have, in the supersonic regime and at the beginning of the mixed regime, the same suction capacities in a given mixer. However, it becomes quite clear that, at low primary generating pressures, the performance of the conical nozzle E is representative of the regimes with separation, whereas the performance of the

doubly curved nozzle  $E_1$  is representative of the pure mixed regimes which are clearly less favorable than the preceding ones.

#### 4.5. Influence of the Position of the Primary Nozzle

The theoretical representation, the experimental verification of which we study here, assumes basically that the primary nozzle discharges into a cylindrical mixer. This is not the only geometrical shape amenable to calculation, because the momentum theorem, on whose application the numerical description of the mixed regime is essentially based, finds a universal simple expression also if it is written between the extreme cross sections of the mixer, in the case where the cross section of the latter develops, so that the pressure along the wall can be considered constant over the entire length separating the planes of reference. This mixing at constant pressure presents perhaps mixed performance superior to that permitted by mixing in a cylindrical stream (ref. 2), but its control is difficult and the construction of the various geometrical configurations is complicated. For this reason we have limited ourselves, in this report, to the study of the simple case of the cylindrical mixer.

Nevertheless, our configurations permitted convenient axial displacement of the primary and secondary ducts with respect to one another and even the eventual withdrawal of the ejection cross section of the primary flow into the secondary settling chamber (fig. 1). Although the geometrical configuration of the arrangement under these conditions no longer conforms to the theoretical representation described, the measured performance does not appreciably differ from that which we are to calculate, at least if the ratio  $\lambda$  is sufficiently large (driving nozzles with small external dimensions). These are the findings indicated in figure 15, which shows the experimental characteristics corresponding to three particular positions of the primary-exit cross section.<sup>5</sup> In contrast, we see in figure 16, obtained under analogous

---

<sup>5</sup>The parameter  $X$ , indicated in figures 15 and 16, marks the position of the plane of the terminal section of the primary nozzle along the axis of the ejector, starting from the abscissa  $X = 0$  indicated in figure 1. As in the calculation of the apparent length  $\xi$  of the mixing tube, the distances are referred to one-fourth of the diameter of the mixing tube. For the mixing tube of small cross section, the primary flow discharges into the secondary convergent tube in the configurations  $0 \leq X < 3.4$ . For  $X > 3.4$ , the contact between the two flows takes place in the cylindrical tube. The experimental results recorded in the various figures of this study correspond, unless noted otherwise, to the position  $X = 4.8$  for the nozzles B, C, D, and, for E and  $E_1$ , to  $X = 2.7$  and  $X = 3.7$ , respectively, with the small and the large mixing tube.

conditions with a nozzle of greater external dimensions, that the modifications in the geometric configuration of the secondary stream caused by the displacement of the nozzle may considerably transform the suction characteristics of the ejector, primarily in the saturated supersonic regimes. In fact, the existence of these mixed regimes does not belong in the scheme of mixing tubes with parallel flows and is encountered in current installations every time when the secondary mass flow is subject to limitation by a geometrically well-defined throat. We perceive here that the displacement of the driving nozzle causes, according to the direction in which it occurs, a change in the cross section of the secondary geometrical throat, favorable or unfavorable to the performance of the configuration.

#### 4.6. Longitudinal Pressure Distributions

The one-dimensional theoretical representation of the supersonic regime assumes that the secondary flow is accelerated along the primary flow and that the appearance of a sonic section limits the secondary mass flow. The pressure condition which we have achieved at the wall of the mixing tube confirms this hypothesis.

Figure 17 represents several longitudinal distributions of the pressure<sup>6</sup> corresponding to different induced mass flows and to the same primary generating pressure sufficiently high to make the supersonic regime prevail for the overall combination of suction characteristics. In the operation at zero induced mass flow, the quasi-periodic distribution of the pressure in the neighborhood of the exit cross section of the primary flow and before the final deenergization of the stream arises from the jet structure itself. It lasts as long as the secondary mass flow is sufficiently weak to make the flow retain the character of a boundary layer. For larger values of the mass flow, the pressure in the secondary flow remains constant and equal to the value  $p''/p_1'' = 0.53$  of the sonic flows.

---

<sup>6</sup>Since the pressure taps at the wall of the mixing tube are not sufficiently numerous to give an accurate picture of the pressure variation, we placed side by side, in figures 17 and 18, the series of test points which correspond, for each type of operation studied, to different neighboring relative positions of the primary nozzle with respect to the mixing tube.



Figure 18 shows, for a lower primary generating pressure, the continued rise of the pressure which characterizes the mixing of the two flows in the mixed regime.

Translated by Mary L. Mahler  
National Advisory Committee  
for Aeronautics

## REFERENCES

1. Mellanby, A. L.: Fluid Jets and Their Practical Applications. Trans. of the Institution of Chem. Eng., VI, 1928, pp. 66-84.
2. Keenan, J. H., Neumann, E. P., and Lustwerk, F.: An Investigation of Ejector Design by Analysis and Experiment. Jour. Appl. Mech., XVII, 3, 1950, pp. 299-309.
3. Johannsen, N. H.: Ejector Theory and Experiments. A. T. S. No. 1, Trans. Danish Acad. Tech. Sci. (Copenhagen), 1951.
4. Fabri, J., Le Grivès, E., and Siestrunk, R.: Etude aérodynamique des trompes supersoniques. Jahrbuch 1953 der Wissenschaftlichen Gesellschaft für Luftfahrt (Braunschweig), 1954, pp. 101-110.
5. Le Grivès, E., Fabri, J., and Paulon, J.: Diagrammes pour le calcul des éjecteurs supersoniques. O.N.E.R.A., Note Tech. No. 35, 1956.
6. Fabri, J., and Siestrunk, R.: Etude des divers régimes d'écoulement dans l'élargissement brusque d'une veine supersonique. Revue générale des Sciences Appliquées, II, 4 (Brussels), 1955, pp. 229-237.
7. Roy, Maurice: Tuyères, trompes, fusées et projectiles - problèmes divers de dynamique des fluides aux grandes vitesses. Pub. No. 203, Pub. Sci. et Tech. du Ministère de l'Air (Paris), 1947.
8. Fabri, J.: Méthode rapide de détermination des caractéristiques d'un écoulement gazeux à grande vitesse. O.N.E.R.A., 17 (Paris), 1949.
9. Von Kármán, Th.: Mechanische Aehnlichkeit und Turbulenz. Nach. Ges. Wiss. Göttingen, Math. Phys. Klasse, 58, 1930. (Available in English translation as NACA TM 611, 1931.)
10. Summerfield, Martin, Foster, Charles R., and Swan, Walter C.: Flow Separation in Overexpanded Supersonic Exhaust Nozzles. Jet Propulsion, vol. 24, no. 5, Sept. - Oct. 1954, pp. 319-321.
11. Crocco, L., and Lees, L.: A Mixing Theory for the Interaction Between Dissipative Flows and Nearly Isentropic Streams. Jour. Aero. Sci., vol. 19, no. 10, Oct. 1952, pp. 649-676.

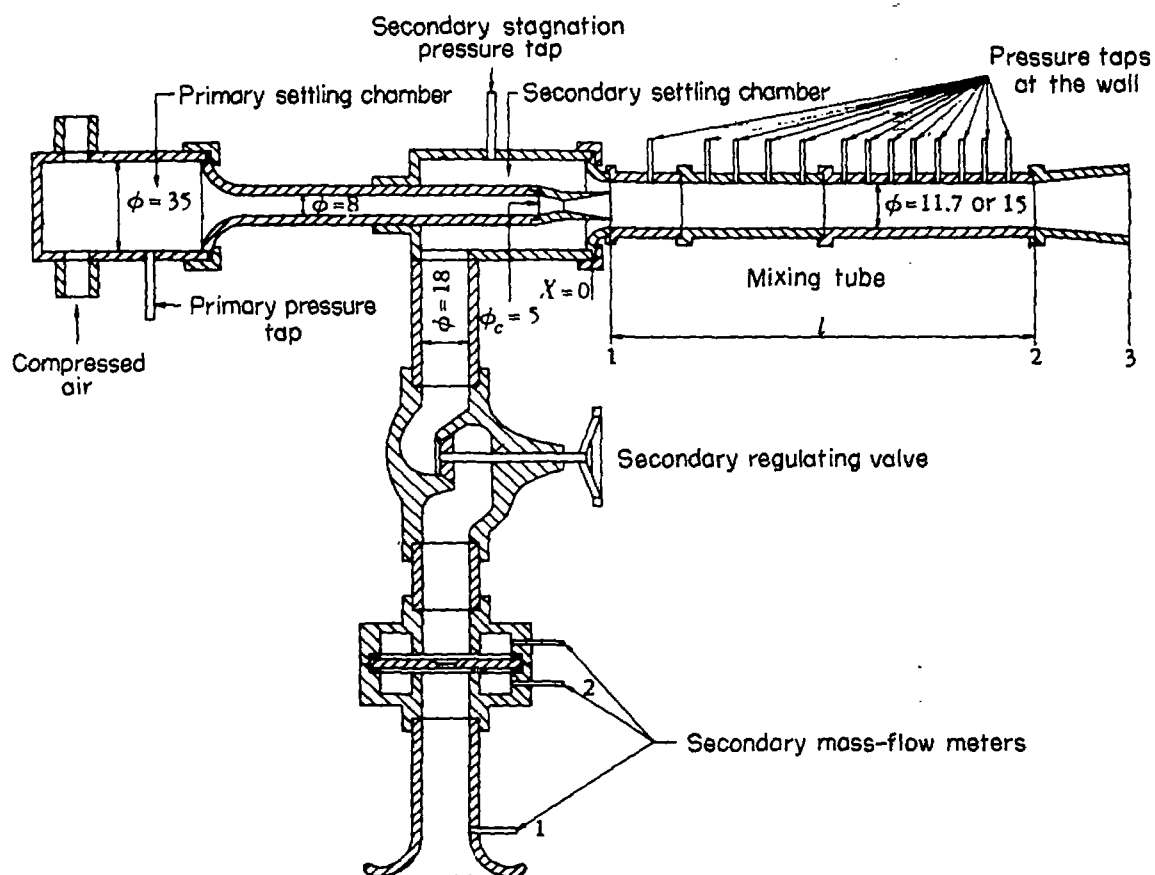


Figure 1.- General diagram of the configuration (dimensions in mm).

	B	C	D	E	E <sub>1</sub>
$M_{*1}'$	1.329	1.545	1.778	1.886	1.886
$\phi_{*}'$	5.01	5.01	5.01	5.02	5.00
$\phi_1'$ int.	5.35	6.06	7.60	8.95	8.90
$\phi_1'$ ext.	5.50	6.40	7.87	9.22	9.50

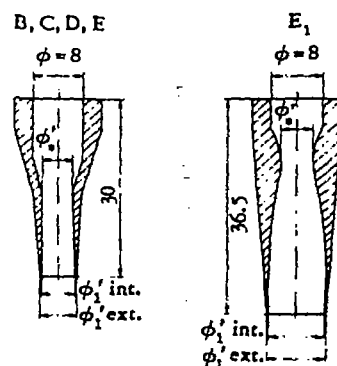
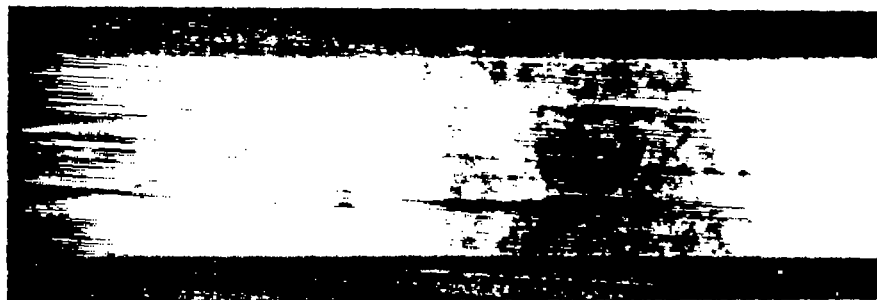
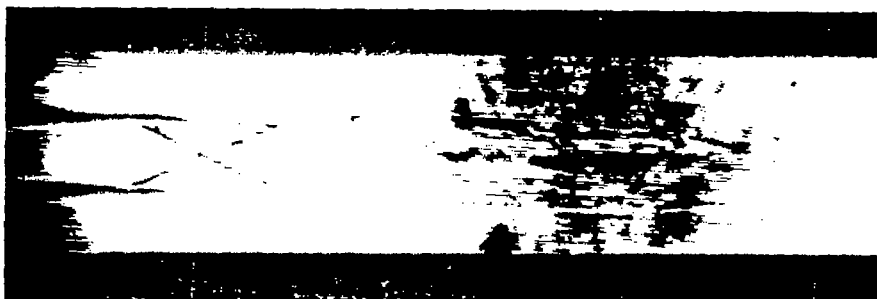


Figure 2.- Characteristic dimensions of the primary nozzles (in mm).



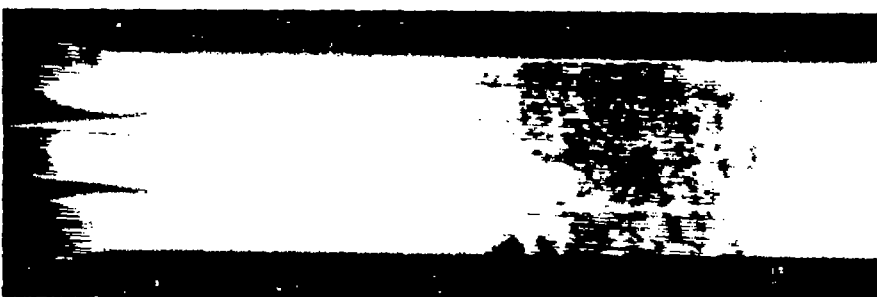
(a) Supersonic regime  $p_1^* = 6p$ ,  $\mu = 0.222$ .



(b) Saturated supersonic regime  $p_1^* = 5p$ ,  $\mu = 0.266$ .



(c) Mixed regime  $p_1^* = 4p$ ,  $\mu = 0.300$ .



(d) Mixed regime with separation  $p_1^* = 3p$ ,  $\mu = 0.445$ .

Figure 3. -



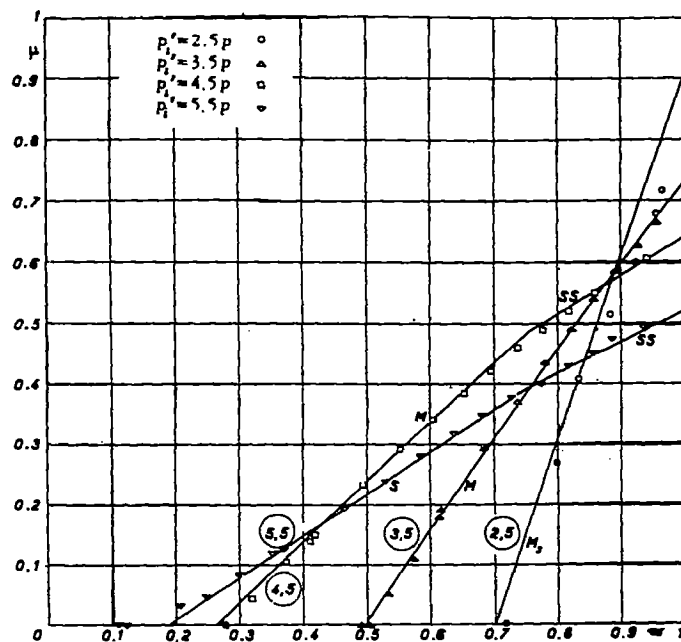


Figure 6.- Comparison of the theoretical and experimental suction characteristics for various primary generating pressures. Nozzle D:  $\lambda_* = 5.454$ ;  $\xi = 61.5$ ;  $\sigma = 1$ .

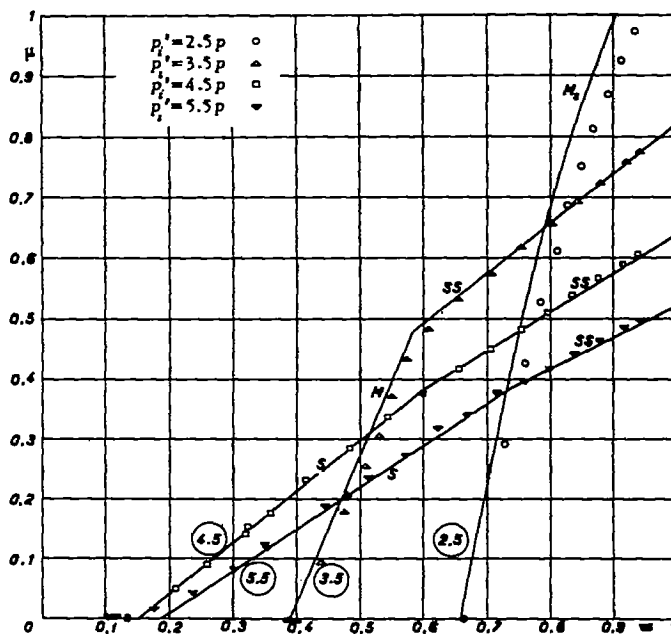


Figure 7.- Comparison of the theoretical and experimental suction characteristics for various primary generating pressures. Nozzle D:  $\lambda_* = 5.454$ ;  $\xi = 61.5$ ;  $\sigma = 2.922$ .

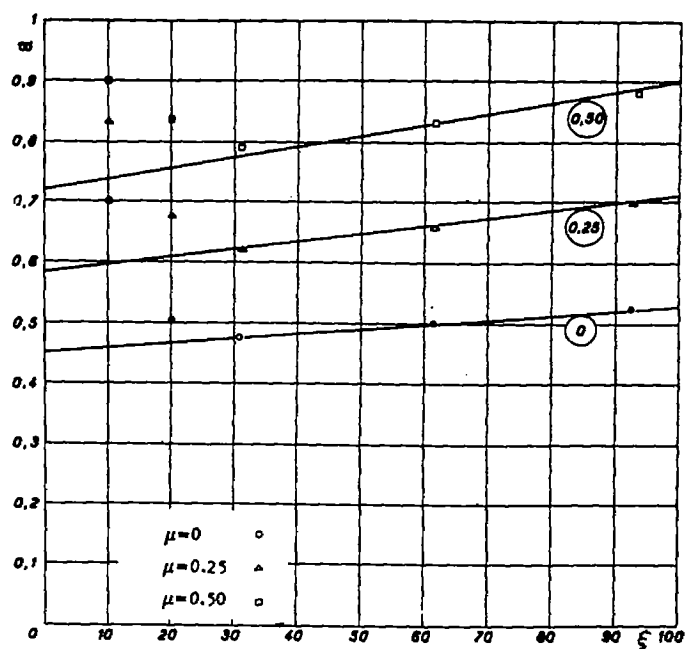


Figure 8. - Variation of the extraction pressure in mixed regime, as a function of the length of the mixing tube for various induced mass flows. Nozzle D:  $\lambda_*$  = 5.454;  $\sigma$  = 1;  $p_1^* = 3.5p$ .

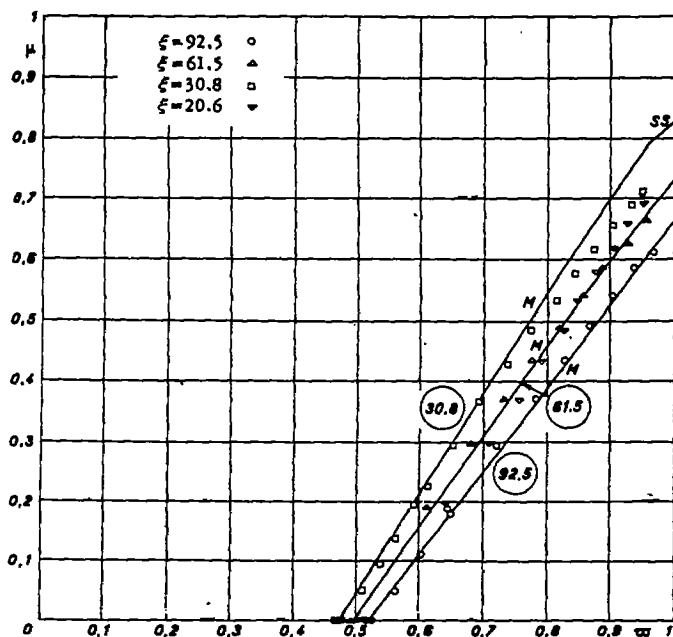


Figure 9(a). - Variation of performance as a function of the length of the mixing tube. Nozzle D:  $\lambda_*$  = 5.454;  $\sigma$  = 1;  $p_1^* = 3.5p$ .

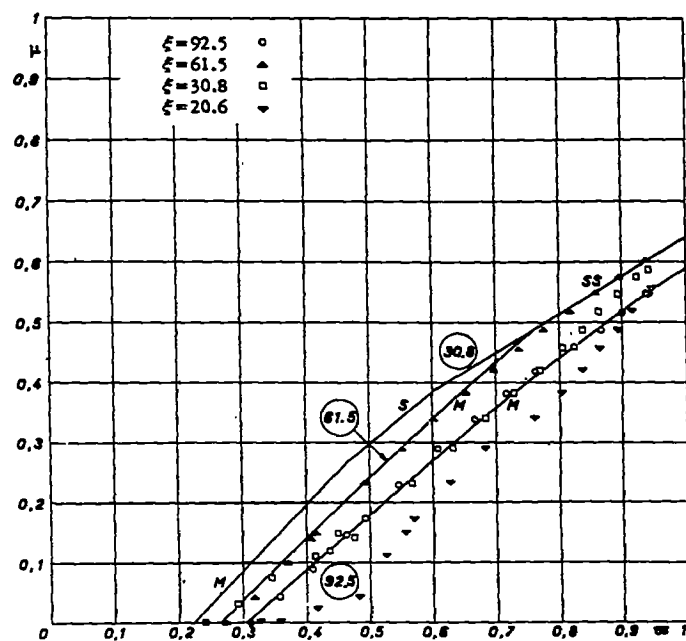


Figure 9(b). - Variation of performance as a function of the length of the mixing tube. Nozzle D:  $\lambda_* = 5.454$ ;  $\sigma = 1$ ;  $p_i = 4.5p$ .

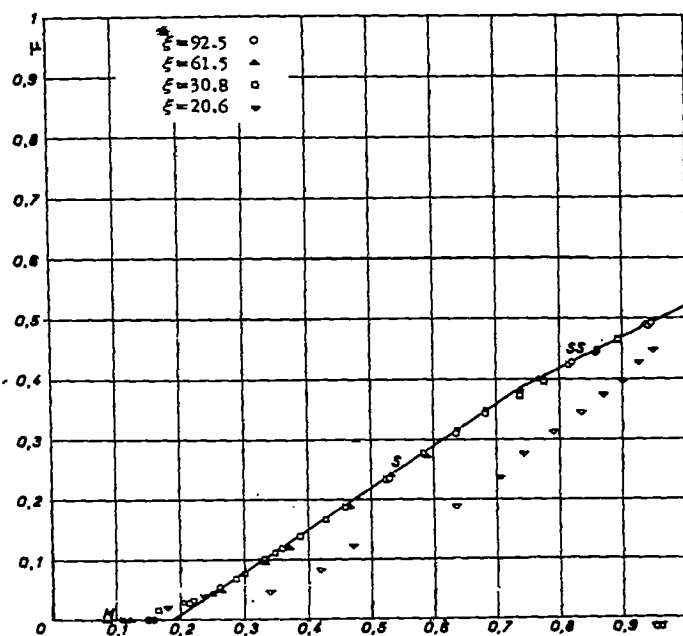


Figure 9(c). - Variation of performance as a function of the length of the mixing tube. Nozzle D:  $\lambda_* = 5.454$ ;  $\sigma = 1$ ;  $p_i = 5.5p$ .



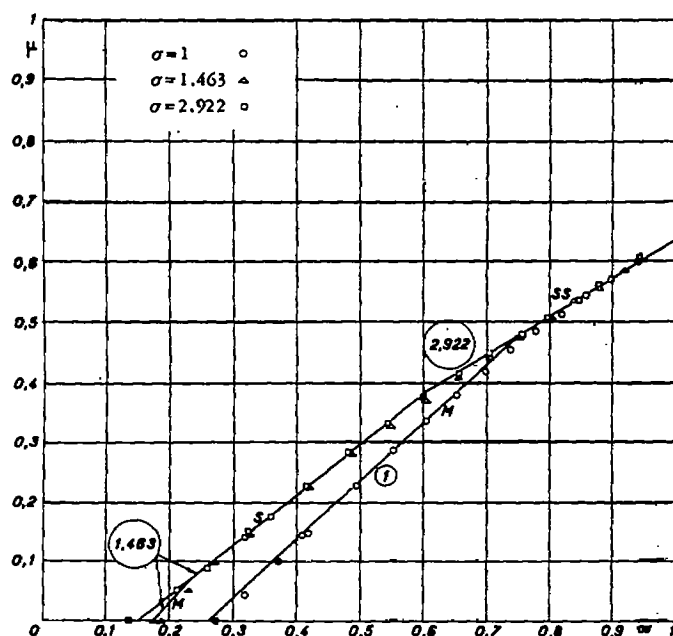


Figure 10.- Variation of performance as a function of the section ratio of the diffuser. Nozzle D:  $\lambda_* = 5.454$ ;  $\xi = 61.5$ ;  $p_1 = 4.5p$ .

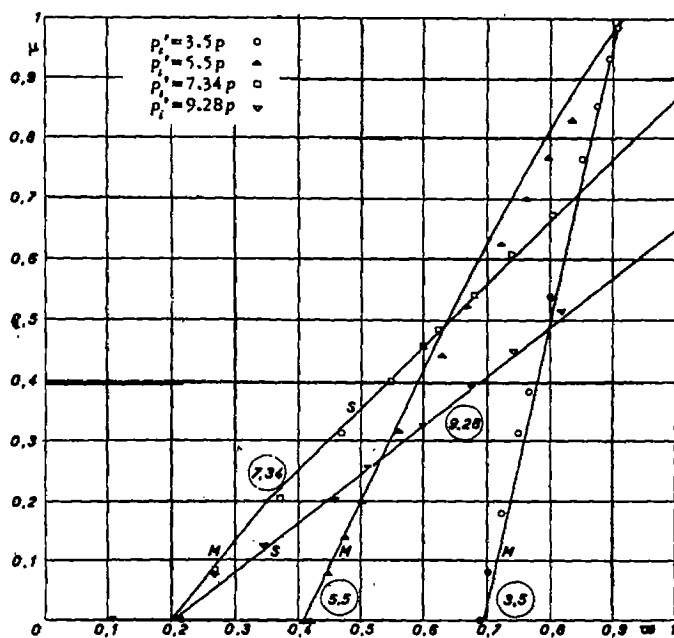


Figure 11.- Variation of performance as a function of the cross section of the mixing tube. (Cf. fig. 6.) Nozzle D:  $\lambda_* = 8.96$ ;  $\xi = 48$ ;  $\sigma = 1$ .

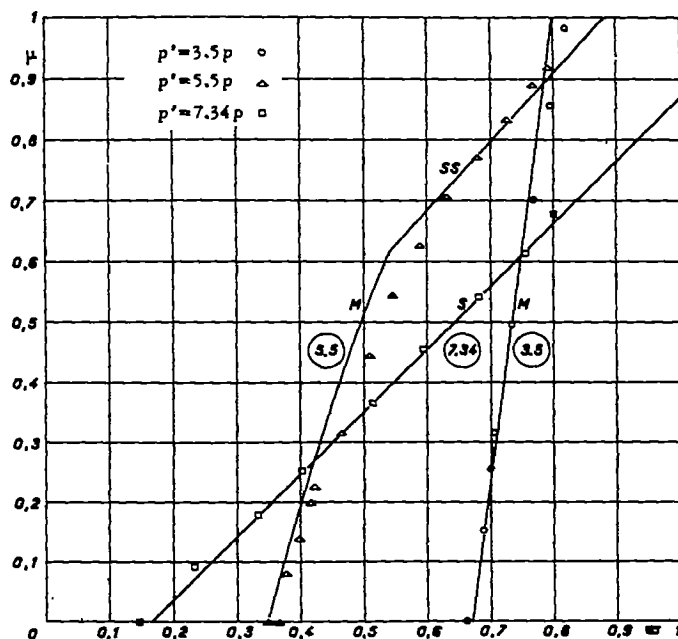


Figure 12.- Variation of performance as a function of the cross section of the mixing tube. (Cf. fig. 7.) Nozzle D:  $\lambda_* = 8.964$ ;  $\xi = 48$ ;  $\sigma = 1.778$ .

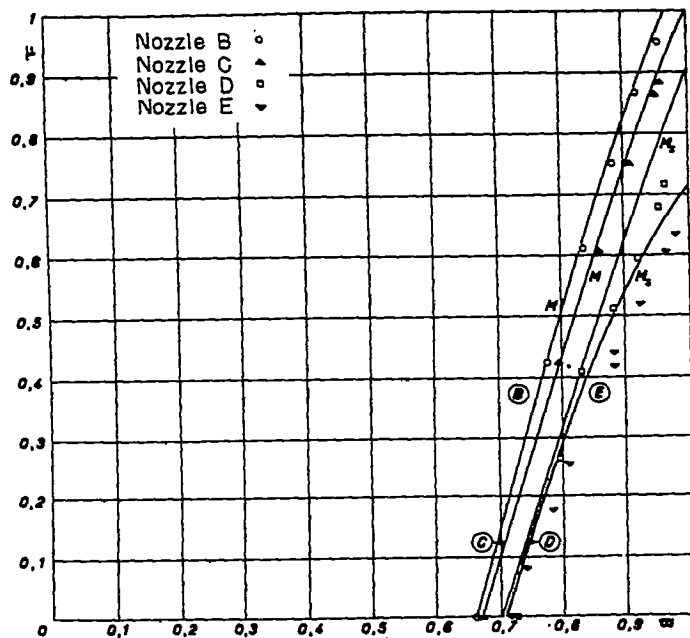


Figure 13(a).- Variation of performance as a function of the primary Mach number. Nozzles B, C, and D:  $\lambda_* = 5.454$ . Nozzle E:  $\lambda_* = 5.432$ ;  $\xi = 61.5$ ;  $\sigma = 1$ ;  $p_1' = 2.5p$ .

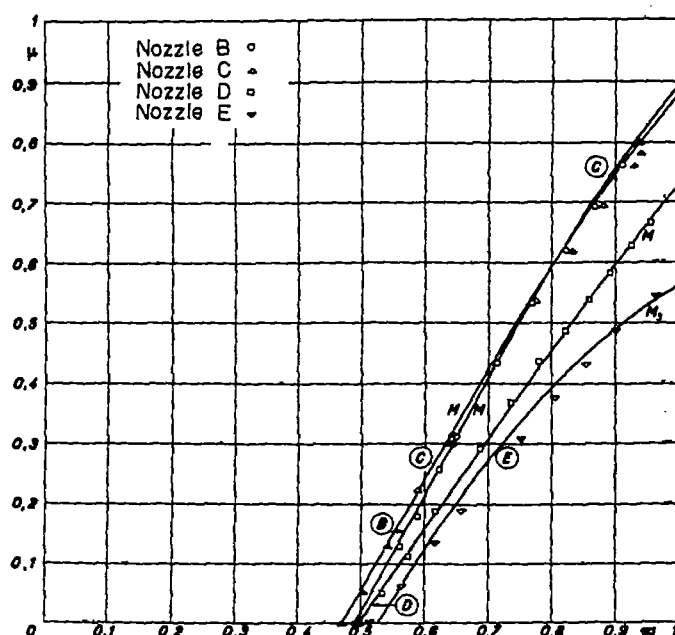


Figure 13(b).- Variation of performance as a function of the primary Mach number. Nozzles B, C, and D:  $\lambda_* = 5.454$ . Nozzle E:  $\lambda_* = 5.432$ ;  $\xi = 61.5$ ;  $\sigma = 1$ ;  $p_1 = 3.5p$ .

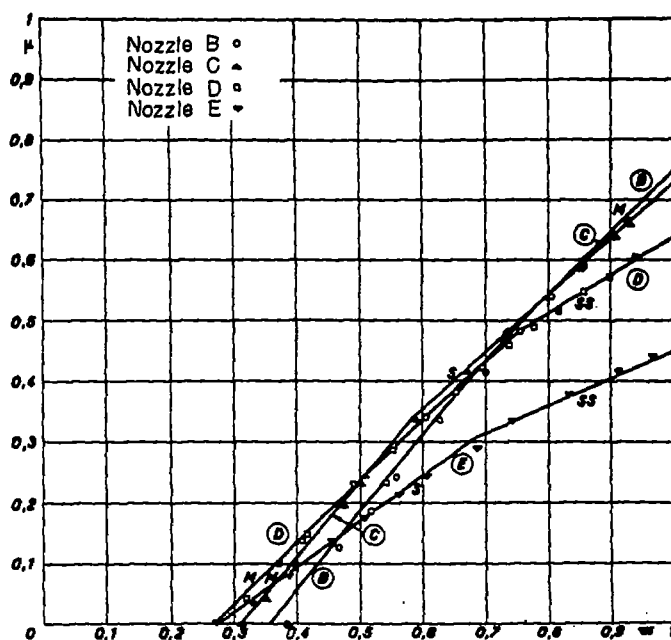


Figure 13(c).- Variation of performance as a function of the primary Mach number. Nozzles B, C, and D:  $\lambda_* = 5.454$ . Nozzle E:  $\lambda_* = 5.432$ ;  $\xi = 61.5$ ;  $\sigma = 1$ ;  $p_1 = 4.5p$ .

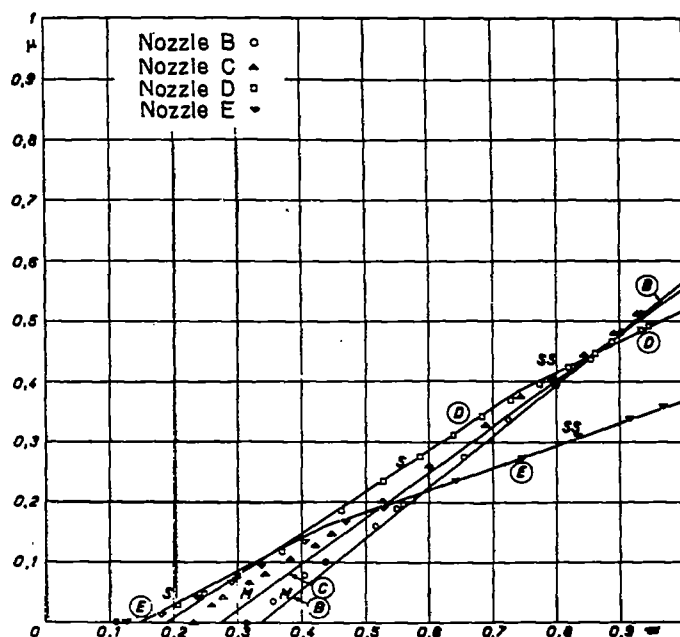


Figure 13(d).- Variation of performance as a function of the primary Mach number. Nozzles B, C, and D:  $\lambda_* = 5.454$ . Nozzle E:  $\lambda_* = 5.432$ ;  $\xi = 61.5$ ;  $\sigma = 1$ ;  $p_1^i = 5.5p$ .

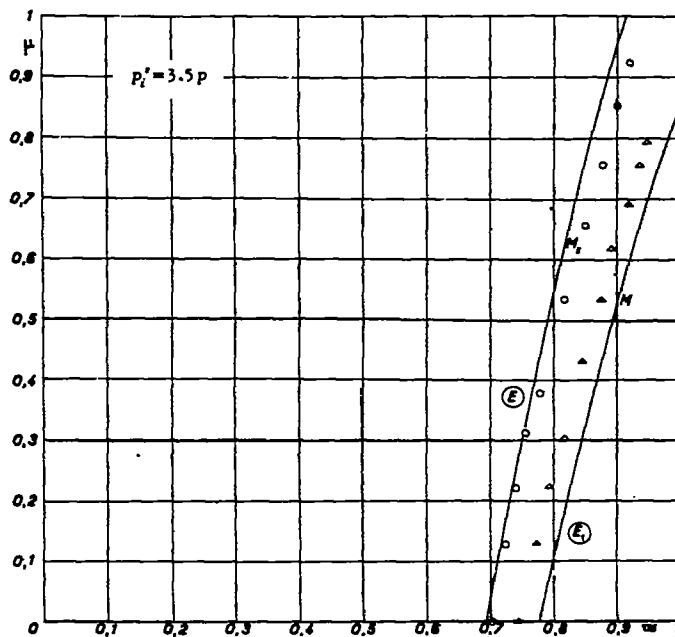


Figure 14(a).- Comparison of mixed performance with or without separation. Nozzle E:  $\lambda_* = 8.928$ . Nozzle E1:  $\lambda_* = 9$ ;  $\xi = 48$ ;  $\sigma = 1$ ;  $p_1^i = 3.5p$ .

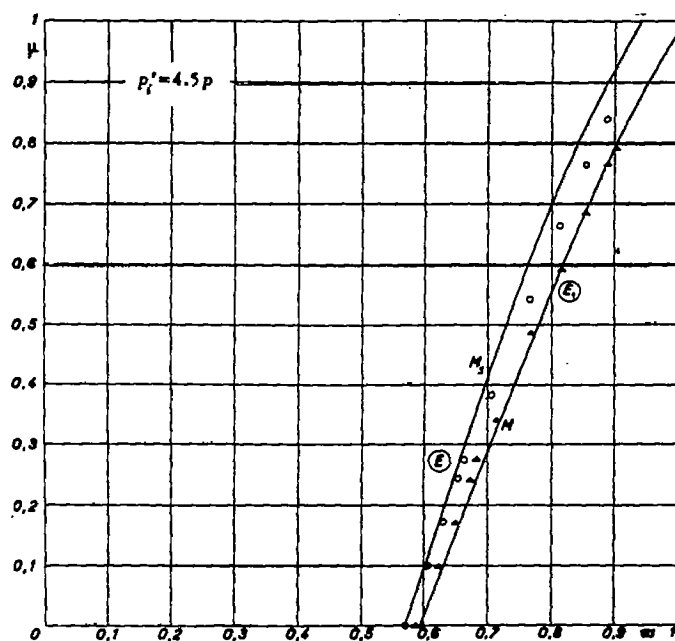


Figure 14(b).- Comparison of mixed performance with or without separation. Nozzle E:  $\lambda_* = 8.928$ . Nozzle  $E_1$ :  $\lambda_* = 9$ ;  $\xi = 48$ ;  $\sigma = 1$ ;  $p'_1 = 4.5p$ .

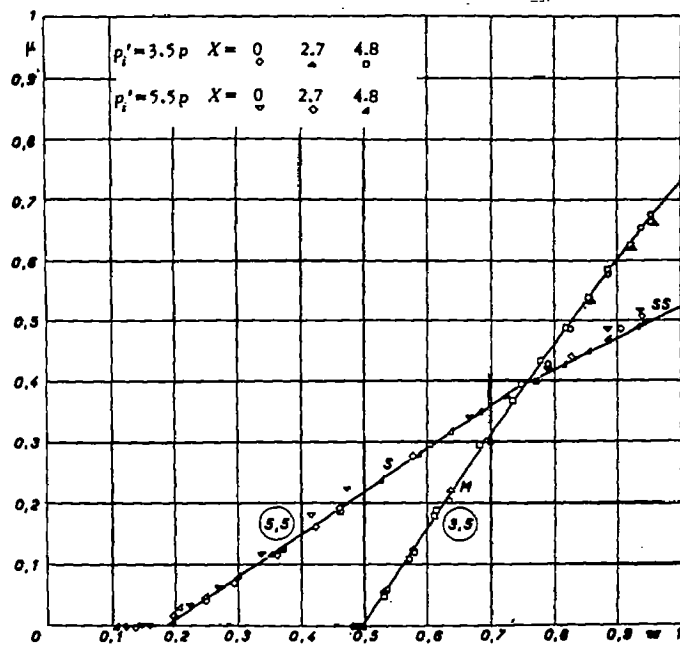


Figure 15.- Variation of performance as a function of the position of the primary nozzle. Nozzle D:  $\lambda_* = 5.454$ ;  $\xi = 61.5$ ;  $\sigma = 1$ .

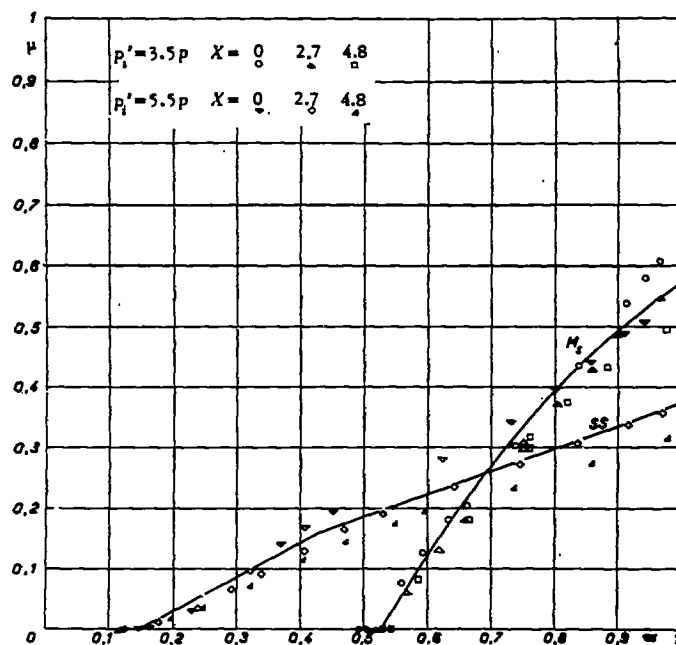


Figure 16.- Variation of performance as a function of the position of the primary nozzle. Nozzle E:  $\lambda_* = 5.432$ ;  $\xi = 61.5$ ;  $\sigma = 1$ .

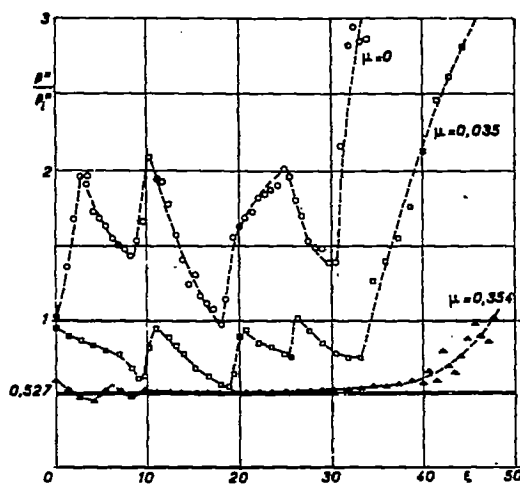


Figure 17.- Distribution of the pressures at the wall of the mixing tube in supersonic regime for different induced mass flows. Nozzle D:  $\lambda_* = 5.454$ ;  $\xi$  total = 61.5;  $\sigma = 1$ ;  $p_1' = 5.88p$ .

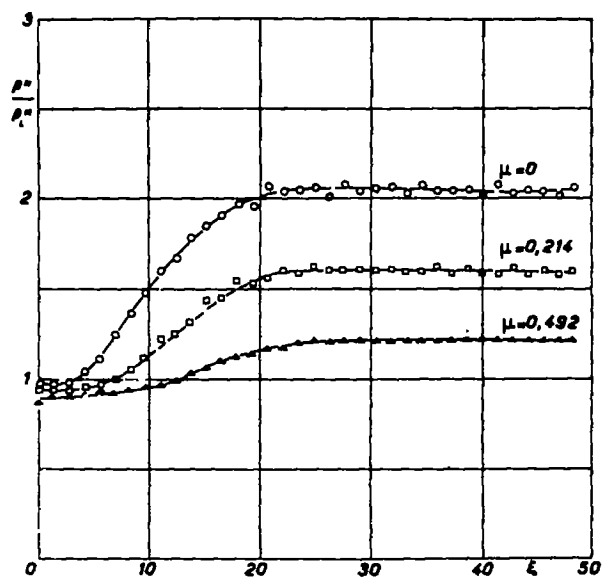


Figure 18.- Distribution of the pressures at the wall of the mixing tube in mixed regime for different induced mass flows. Nozzle D:  $\lambda_* = 5.454$ ;  $\xi_{\text{total}} = 61.5$ ;  $\sigma = 1$ ;  $p_1^* = 3.54p$ .